Methods xxx (xxxx) xxx–xxx

Contents lists available at ScienceDirect

Methods

journal homepage: www.elsevier.com/locate/ymeth

Synthesis of multi-omic data and community metabolic models reveals insights into the role of hydrogen sulfide in colon cancer

Vanessa L. Hale[a,b,c], Patricio Jeraldo[b,c], Michael Mundy[d], Janet Yao[b], Gary Keeney[e], Nancy Scott[e], E. Heidi Cheek[e], Jennifer Davidson[e], Megan Green[e], Christine Martinez[e], John Lehman[e], Chandra Pettry[e], Erica Reed[e], Kelly Lyke[c], Bryan A. White[f], Christian Diener[g], Osbaldo Resendis-Antonio[g,h], Jaime Gransee[i], Tumpa Dutta[i], Xuan-Mai Petterson[i], Lisa Boardman[j], David Larson[c], Heidi Nelson[b,c], Nicholas Chia[b,c,*]

[a] Department of Veterinary Preventative Medicine, The Ohio State University College of Veterinary Medicine, Columbus, OH, USA
[b] Microbiome Program, Center for Individualized Medicine, Mayo Clinic, Rochester, MN, USA
[c] Department of Surgery, Mayo Clinic, Rochester, MN, USA
[d] Center for Individualized Medicine, Mayo Clinic, Rochester, MN, USA
[e] Division of Laboratory Medicine and Pathology, Mayo Clinic, Rochester, MN, USA
[f] Carl R. Woese Institute for Genomic Biology, Department of Animal Sciences, Division of Nutritional Sciences, University of Illinois, Champaign-Urbana, IL, USA
[g] Human Systems Biology Laboratory, National Institute of Genomic Medicine, Mexico City, Mexico
[h] Coordinación de la Investigación Científica, Red de Apoyo a la Investigación, UNAM, Mexico City, Mexico
[i] Mayo Clinic Metabolomics Core Laboratory, Mayo Clinic, Rochester, MN, USA
[j] Division of Gastroenterology and Hepatology, Mayo Clinic, Rochester, MN, USA

A B S T R A C T

Multi-omic data and genome-scale microbial metabolic models have allowed us to examine microbial communities, community function, and interactions in ways that were not available to us historically. Now, one of our biggest challenges is determining how to integrate data and maximize data potential. Our study demonstrates one way in which to test a hypothesis by combining multi-omic data and community metabolic models. Specifically, we assess hydrogen sulfide production in colorectal cancer based on stool, mucosa, and tissue samples collected on and off the tumor site within the same individuals. 16S rRNA microbial community and abundance data were used to select and inform the metabolic models. We then used MICOM, an open source platform, to track the metabolic flux of hydrogen sulfide through a defined microbial community that either represented on-tumor or off-tumor sample communities. We also performed targeted and untargeted metabolomics, and used the former to quantitatively evaluate our model predictions. A deeper look at the models identified several unexpected but feasible reactions, microbes, and microbial interactions involved in hydrogen sulfide production for which our 16S and metabolomic data could not account. These results will guide future *in vitro*, *in vivo*, and *in silico* tests to establish why hydrogen sulfide production is increased in tumor tissue.

1. Introduction

Integration of multi-omic data has become increasingly important as studies of the microbiome have advanced and as our understanding of microbial community dynamics continues to grow. In the gut, for example, it is now appreciated that microbial interactions and community function may play a more important role than single microbes in some disease processes including *Clostridium difficile* infection [1], Type 2 diabetes [2], and atherosclerosis [3]. As such, the tools and techniques for studying microbial metabolites and interactions are rapidly developing, and the integration of multi–omic data is increasingly feasible on many platforms. Data integration using statistical correlations between microbiome and metabolome [4–6] or metatranscriptome and metagenome [7,8] has given us unique insights into gut microbial ecology and disease processes. However, correlation does not imply causation and cannot uncover underlying biological mechanisms. Mechanistic

Abbreviations: CRC, Colorectal Cancer; GEMs, Genome Scale Metabolic Models; GC–MS, Gas Chromatography–Mass Spectrometry; LC-MS, Liquid Chromatography–Mass Spectrometry; UPLC-MS, Ultra Pressure Liquid Chromatography–Mass Spectrometry; SCFA, Short Chain Fatty Acid

* Corresponding author at: Harwick 3-21, Mayo Clinic, 200 1stSt SW, Rochester, MN 55902, United States.
E-mail address: chia.nicholas@mayo.edu (N. Chia).

https://doi.org/10.1016/j.ymeth.2018.04.024
Received 12 October 2017; Received in revised form 5 March 2018; Accepted 22 April 2018

modeling, on the other hand, offers a way to examine data through the lens of biological interaction; and microbes, metabolites, or reactions of interest in the models can be queried and further analyzed [9]. In this study, we characterize an approach for integrating multi-omic data that uses the principles of metabolic model reconstruction and modeling in order to examine a specific mechanistic hypothesis that relates microbial hydrogen sulfide production and colorectal cancer (CRC).

CRC is the one of the leading causes cancer death in the United States [10]. It has also been linked to alterations in the gut microbiome and metabolome [11]. The microbially-produced metabolites implicated in CRC development or progression include hydrogen sulfide [12], reactive oxygen species [13], *N*-nitroso compounds [14,15], polyamines [16], and secondary bile acids [17,18]. Adding to this complex landscape, it appears that the effects of some metabolites are context dependent. Butyrate, a short chain fatty acid (SCFA), is reportedly both an inducer [19] and an inhibitor [20] of CRC tumor development. Hydrogen sulfide, which has been implicated in our work and others' [12,21–23], is a genotoxic and cytotoxic agent at physiologic concentrations [13,24,25], but it has also been reported as an anti-inflammatory and potentially anti-tumor agent [26–30].

Quantifying the concentration of hydrogen sulfide in the gut is inherently difficult given its volatile nature [31]. In contrast, quantifying the relative abundance of hydrogen sulfide-producing bacteria is far less challenging. Sulfidogenic bacteria such as *Bilophila wadsworthia*, *Fusobacterium* species, and sulfur-reducers such as *Desulfovibrio* species have all been identified within the gut and linked to colon inflammation [32], adenomas [21,33,34], and colon tumors [35–37]. However, these microbial associations are not sufficient for determining microbial metabolite production. Examining the effects of single microbes on CRC fails to capture microbial interactions or community effects that may alter the rate of hydrogen sulfide production and subsequent pathogenesis. Investigations on the role of microbial metabolites in CRC requires an approach capable of capturing metabolite production within the context of different microbial communities.

Microbial metabolic models and the tools built around these models provide an opportunity to examine microbial community interactions [38–40] and test the relationship between microbial hydrogen sulfide production and CRC. Genome-scale metabolic models (GEMs) are reconstructed metabolic networks based on complete annotated genome sequences [41]. GEMs can be used to calculate reaction fluxes for a specific target function—e.g., growth—by optimizing metabolite flow through a metabolic network [42]. Recently developed tools allow users to assess pairwise (e.g. MMINTE [38]) or community interactions (e.g. MICOM [40,43]) between microbial GEMs. Unlike correlations which identify pairs of microbes and metabolites that are concurrently increased or decreased, community metabolic modeling tools like MICOM capture more complex microbial interactions such as cross-feeding and resource competition. Additionally, the flux of specific metabolites (i.e. hydrogen sulfide) or specific reactions (i.e. cysteine degradation) can be tracked in these models.

In this study, we obtained 16S microbial community data from colon tissue, mucosa, and stool samples in individuals diagnosed with colorectal cancer. Samples were collected at the tumor site and at adjacent normal (hereafter referred to as "adjacent") and distant normal (hereafter referred to as "normal") colon sites. 16S data was then used to select and inform genome-scale metabolic models that represented "tumor," "adjacent," and "normal" microbial communities. Metabolite abundances were inferred by tracking metabolic flux in MICOM. Models were also queried to identify specific microbes and reactions contributing to these fluxes. Targeted and untargeted metabolomics on colon tissue were performed to validate model predictions. The synthesis of modeling and experimental results here provided an improved means to maximize data potential, test a specific hypothesis about hydrogen sulfide production, and gain unexpected insights into microbial community behavior in CRC. Specifically, our models predict increased hydrogen sulfide flux in CRC tumors tissue attributed to *Fusobacterium nucleatum*, *Clostridium perfringens,* and *Filifactor alocis*.

Table 1
Demographics of individuals with colorectal cancer.

	Subgroups
Sex(n,%)	Males 57 (53.89%)
	Females 49 (46.2%)
Age (mean,range)	65.3 (23–90)
BMI (mean,range)	27.7 (16–54.8)
Any history of smoking?	Yes 58 (54.7%)
	No 48 (45.3%)
Cancer stage (n, %)	1, 21 (19.8%)
	2, 27 (25.5%)
	3, 40 (37.7%)
	4, 6 (5.7%)
	Unknown,12 (11.3%)
Colon tumor location(n, %)	right side 36(34%)
	left side 58 (54.7%)
	transverse 11 (10.4%)
	multiple 1 (0.9%)

2. Methods

2.1. Human subject enrollment

This study was approved the Mayo Clinic Institutional Review Board (IRB# 14-007237 and IRB# 622-00). Adults (> 18 years old) who were identified as being surgical candidates for colorectal cancer (n = 106) were voluntarily enrolled at Mayo Clinic in Rochester, Minnesota (Table 1; for tumor location by cancer stage: Supp. Table 1). Exclusion criteria included radiation therapy or chemotherapy in the 2 weeks prior to enrollment. (For a complete list of patient medications at the time of surgery see Supp. Table 2.) Patients with lower anterior resections or a diverting ileostomy were additionally prescribed a MiraLAX bowel preparation. Immediately prior to surgery, all patients received tap water or MiraLAX enemas. Partial or total colectomies were performed on each patient and, as feasible, colon tissue, mucosal scrapes, and stool samples (fecal material in contact with colon tissue) were obtained from the tumor site, adjacent normal area ("adjacent"), and distant normal area ("normal"). Mucosal scrapes and a portion of each tissue sample (~1 cm^2 of full thickness colon tissue) was immediately snap frozen in TE buffer (10 mmol Tris, 1 mmol EDTA, pH 8). A separate sample of tumor tissue was preserved in formalin and submitted to pathology. Stool collected from within the colon at surgery was frozen without a buffer at -80 °C until DNA extraction.

2.2. DNA extraction and 16S rRNA gene sequencing

Stool DNA extraction [21], quantification, and amplification was performed as described previously [44]. Colon tissue was thawed, weighed, and homogenized prior to DNA extraction. Mucosal scrape samples were centrifuged; the supernatant was removed, and the pellet was used for DNA extraction. Colon tissue and mucosal scrape DNA extraction was performed using the Mo Bio PowerSoil DNA isolation kit (Mo Bio Laboratories, A Qiagen Company, Carlsbad, CA, USA). Library preparation on all samples was performed at the Mayo Clinic Microbiome Lab (Rochester, MN) and sequencing was completed at the Mayo Clinic Medical Genomics Facility using a MiSeq instrument (2 × 300, 600 cycles, Illumina Inc.)

2.3. DNA sequence processing and analysis

Sequencing data was processed as previously described [44,45]. In brief, the IM-TORNADO bioinformatics pipeline was used to assign paired sequences at a 97% identity match to operational taxonomic units (OTUs) [45]. Taxonomy assignment was made using the

Ribosomal Database Project (RDP) version 9 [46]. Samples ranged from 0 to 514, 568 reads after processing. All samples with < 500 reads were excluded from analyses. No-template control samples were included with each group of samples that underwent extraction. Positive and no-template controls were also included during PCR amplifications. OTUs identified as contaminants present in no-template control samples were removed from analyses. Analyses including alpha- and beta-diversity and Kruskal-Wallis significance testing (group_significance.py in QIIME) were performed in QIIME 1.9.1 [47] and R 3.4.1. In order to achieve adequate statistical power, all samples, regardless of tumor location and stage were combined in our analyses. 16S sequencing data can be found at the NCBI Sequence Read Archive under BioProject accession PRJNA445346. Metagenomic sequencing data can be found at the NCBI Sequence Read Archive under BioProject accession PRJNA397219.

2.4. Real-time PCR for detection of Bacteroides fragilis toxin gene

Real-time PCR was performed on a QuantStudio 6 Flex Real-Time PCR System (Applied Biosystems, Waltham, MA, USA), and stool DNA was tested for the presence or absence of the *Bacteroides fragilis* toxin (bft) genes. For detection of the bft gene, PCR amplification was performed using primers BFT-F (5′-GGATAAGCGTACTAAAATACAGCTG GAT-3′), BFT-R (5′-CTGCGAACTCATCTCCCAGTATAAA-3′) and the probe (5′-FAM-CAGACGGACATTCTC-NFQ-MGB-3′) [48]. Toxigenic *B. fragilis* (ATCC 43858, ATCC, Manassa, VA, USA) was used as a positive control. PCR was performed using 10 µl of TaqMan Universal Master Mix II (2X), no UNG (Applied Biosystems, Waltham, MA, USA) combined with 900 nM of each primer and 250 nM of the probe. Sterile water was added to adjust the final reaction volume to 20 µl. Cycling parameters were 95 °C for 10 min then 50 cycles of 95 °C for 15 s and 60 °C for 20 s.

2.5. Metabolomics sample preparation and analysis

2.5.1. Tissue sample preparation

Colon tissue and mucosal scrape tissue were removed from TE buffer, rinsed in ice cold PBS, pulverized with a frozen mortar and pestle and stored at -80 °C until submission for targeted and untargeted analysis.

2.5.2. Amino acid panel on UPLC-MS

Serine, homoserine, lanthionine and cystathionine – all amino acids produced concurrently with and proxies for hydrogen sulfide – were measured by LC-MS, similar to our amino acid plus metabolites panel as referenced [49]. Tissue homogenate samples were spiked with internal standards (10 µl of serine, homserine, lanthionine, and cystathionine each at a concentration of 2 µg/ml), then deproteinized with cold methanol followed by centrifugation at 10,000*g* for 15 min. The supernatant was immediately derivatized with 6-aminoquinolyl-N-hydroxysuccinimidyl carbamate according to Waters' MassTrak kit. An 11-point calibration curve underwent similar derivatization procedure after the addition of internal standards. Both derivatized standards and samples were analyzed on a triple quadrupole mass spectrometer (Thermo TSQ Quantum Ultra) coupled with an Ultra Pressure Liquid Chromatography (Waters Acquity) system. Data acquisition was done using select ion monitor (SRM). The following transitions (*m/z*) were monitored: 276.25 > 171.04 for serine, 290.2 > 171.04 for homoserine, 275.2 > 171.04 for lanthionine and 282.3 > 171.04 for cystathionine. Concentrations of the analytes of each unknown were calculated against each respective calibration curve.

2.5.3. Short chain fatty acids (SCFA) panel on GC–MS

SCFA were quantitated via GC–MS as previously published with a few modifications [50]. Briefly, 50 µl tissue homogenate was added to a tube containing internal standard (2 µl of 2-ethylbutyric acid at a concentration of 9 µg/ml) in HCl. One milliliter of dichloromethane (DCM) was used to extract SCFA from the mixture. The extract was derivatized with N-Methyl-N-*tert*-butyldimethylsilyltrifluoroacetamide (MTBSTFA) prior to analysis on GC–MS. Concentrations of acetic acid (*m/z* 117.0), propionic acid (*m/z* 131.1), isobutyric acid (*m/z* 145.1), butyric acid (*m/z* 145.1), isovaleric acid (*m/z* 159.1), valeric acid (*m/z* 159.1), isocaproic acid (*m/z* 173.2) and hexanoic acid (*m/z* 173.2) were measured against 11-point calibration curves that underwent the same derivatization.

2.5.4. Data analysis of targeted metabolomics

Kruskal-wallis or ANOVA significance testing followed by Dunn's post hoc tests were performed in R 3.4.1 to assess metabolite differences between tumor, adjacent, and normal tissue. All samples, regardless of tumor location and stage were combined in our analyses.

2.5.5. Qualitative large-scale profiling on LC-MS – untargeted metabolomics

Tissue homogenates (50 µl) were deproteinated with cold acetonitrile: methanol (1:6 ratio), kept on ice with intermittent vortexing and centrifuged at 18000 × *g* for 30 min at 4 °C. $^{13}C_6$-phenylalanine (3 µl at 250 ng/µl) was added as internal standard to samples. The supernatant was divided into 4 aliquots and dried down using a stream of nitrogen gas for analysis on a Quadruple Time-of-Flight Mass Spectrometer (Agilent Technologies 6550 Q-TOF) coupled with an Ultra High Pressure Liquid Chromatograph (1290 Infinity UHPLC Agilent Technologies). Profiling data was acquired under both positive and negative electrospray ionization conditions over a mass range *m/z* of 100–1700 at a resolution of 10,000 (separate runs) in scan mode. Metabolite separation was achieved using two columns of differing polarity, a hydrophilic interaction column (HILIC, ethylene-bridged hybrid 2.1 x 150 mm, 1.7 µm; Waters) and a reversed-phase C18 column (high-strength silica 2.1 × 150 mm, 1.8 µm; Waters) with gradient described previously [51–53]. Run time was 18 min for HILIC and 27 min for C18 column using a flow rate of 400 µl/min. A total of four runs per sample were performed to give maximum coverage of metabolites. Samples were injected in duplicate, wherever necessary, and a pooled quality control (QC) sample, made up of all of the samples from each study was injected several times during a run. A separate plasma quality control (QC) sample was analyzed with pooled QC to account for analytical and instrumental variability. Dried samples were stored at -20 °C until analysis. Samples were reconstituted in running buffer and analyzed within 48 h of reconstitution. Auto-MS/MS data was also acquired with pooled QC sample to aid in unknown compound identification using fragmentation pattern.

2.5.6. Data analysis of untargeted metabolomics

Data alignment, filtering, univariate, multivariate statistical and differential analysis was performed using Mass Profiler Professional (Agilent Inc, Santa Clara, CA, USA). Metabolites detected in at least ≥ 80% of one of two groups were selected for differential expression analyses. Metabolite peak intensities and differential regulation of metabolites between groups were determined as described previously [51,53]. Each sample was normalized to the internal standard and log 2 transformed. Unpaired *t*-test with multiple testing correction $p < 0.05$ was used to find metabolites significantly different between the two groups. Default settings were used with the exception of signal-to-noise ratio threshold (3), mass limit (0.0025 units), and time limit (9 s). Putative identification of each metabolite was done based on accurate mass (*m/z*) against METLIN database using a detection window of ≤7 ppm. The putatively identified metabolites were annotated as Chemical Abstracts Service (CAS), Kyoto Encyclopedia of Genes and Genomes (KEGG), Human Metabolome Project (HMP) database, and LIPID MAPS identifiers [54].

Significance testing of identified and unidentified compounds by sample type (tumor, adjacent, normal) was performed using one-way ANOVA followed by TukeyHSD post hoc tests. P-value computations

were asymptotic and the Benjamini-Hochberg correction was used for multiple testing. All samples, regardless of tumor location and stage were combined in our analyses.

2.6. Community metabolic modeling

To model the metabolism of the bacterial communities detected in the tissue samples, we used the MICOM tool, which constructs a steady-state community model based on a set of individual genome-scale metabolic models of bacteria and their relative abundances. Notably, a steady-state model may not provide the most effective representation of the dynamic gut community. However, intra-individual gut microbial composition and diversity is, in fact, relatively stable over the long-term (years) [55]; thus, we used the model assumptions and proceeded with our analyses as follows: We used the AGORA set of individual metabolic models [56] for bacteria. We matched the 16S rRNA gene sequence of each OTU of our dataset to the 16S rRNA genes identified in the genomes used to construct the AGORA models. In the cases where the 16S rRNA genes were not identified in the genomes, we either looked up the corresponding sequence in Genbank, or, if possible, re-assembled the genomes from publicly deposited data using SPAdes 3.11.0 [57] through Unicycler 0.4.1 [58]. For matching the OTU sequences to the AGORA 16S sequences, we used VSEARCH 2.4.3 [59] with minimum identity of 97%, and parameters maxaccepts 0 and maxrejects 0, selecting the model sequence with highest identity. In case of multiple top matches, the first model in database order is selected. Then the model is assigned the relative abundance for the corresponding OTU in a particular sample. For multiple OTUs mapping to a single model, their relative abundances were added. We also calculated the abundance fraction explained by the set of models. For each sample, we then proceed to run the MICOM tool inputting the models to use and their relative abundances. As media condition, we used a complete medium with the exchange flux for O2 set to zero (EX_o2_m = 0), to replicate anaerobic conditions. If present, we also knocked out the following reactions from an *Escherichia coli* model (Escherichia_coli_str_K_12_substr_MG1655): CYSDS, FXXRDO and SULR. MICOM finally optimized the fluxes using its “linear lagrangian” method, with the GNU Linear Programming Kit (GLPK) as the solver backend, obtaining a table of microbe growth rates and reaction fluxes as output for analysis. Predicted hydrogen sulfide flux through the community metabolic models was quantified in tumor, adjacent, and normal tissue. Any samples that fell outside of the 95% confidence intervals of hydrogen sulfide flux were removed as outliers.

Pearson correlations were used to assess the direct relationship between predicted flux of hydrogen sulfide through community metabolic models and amino acid concentrations from metabolomics. Models were then queried to identify microbes and reactions responsible for hydrogen sulfide flux.

3. Results

3.1. Microbial composition and diversity

From 16S sequencing, we obtained an average of 41,271 and 5792 paired reads per sample before and after quality control filtering respectively. The microbial composition and diversity of colon tissue, stool, and mucosa were examined in relation to sample type: tumor, adjacent, or normal. Alpha-diversity, or within sample microbial diversity, was significantly lower in tumor tissue samples as compared to adjacent and normal tissue samples (Fig. 1, Supp. Fig. 1). No distinct clustering was noted by sample type based on weighted (Fig. 2) or unweighted (Supp. Fig. 2) principal coordinate analysis (PCoA) of beta-diversity. Despite this, 18 microbes were identified as differentially abundant based on sample type (Supp. Table 3). Notably, a hydrogen-sulfide-producing OTU identified as a *Fusobacterium* species was the only OTU significantly enriched in the tumor samples. *Fusobacterium* along with *Bacteroides fragilis* were also identified as significantly enriched in early stage (stage 1 and 2) tumor tissue samples as compared to late stage (stage 3 and 4) samples (Supp. Table 4). We next wanted to determine if the *B. fragilis* we were observing in our samples was toxigenic or not, as toxigenic *B. fragilis* has a well-established link to CRC [60,61]. qPCR for the bft gene on stool DNA samples identified toxigenic *B. fragilis* in 9 out of the 98 (9.2%) individuals we tested (Supp. Table 5).

3.2. Metabolite profiles

To examine the metabolic environment in the gut, we performed targeted and untargeted metabolomics. Despite relatively few microbial compositional differences between tumor, adjacent, and normal samples, analyses of untargeted metabolomic profiles identified clear metabolic differences in tumor tissue samples as compared to adjacent or normal tissue samples (Fig. 3). Over 124 identified compounds (Supp. Table 6) and over 111 unidentified compounds (Supp. Table 7) were found to be significantly enriched in tumor tissue.

To test more specifically for hydrogen sulfide production, we quantified 4 amino acids (serine, homoserine, lanthionine, and cystathionine) concurrently produced with hydrogen sulfide (Fig. 4). These amino acids are less volatile and easier to quantify than gaseous hydrogen sulfide. Of these metabolites, lanthionine and cystathionine are the most specific proxies for hydrogen sulfide as serine and homoserine are also produced in other non-hydrogen-sulfide producing pathways. Lanthionine, cystathioine, and homoserine were all significantly enriched in tumor tissue (Fig. 5), suggesting increased hydrogen sulfide production on the tumor. We also quantified short chain fatty acid (SCFA) levels in colon tissue but did not find any significant differences in SCFAs on or off tumor (Supp. Fig. 3).

3.3. Community metabolic modeling

To evaluate how microbial community metabolic interactions could be shaping the metabolic environment – particularly in relation to hydrogen sulfide production, we used 16S microbial composition and abundance data to construct genome-scale metabolic models that represented the communities associated with tumor, normal, and adjacent tissue samples. After performing flux balance analysis on the communities using MICOM, we then examined the results for hydrogen sulfide flux. Tumor tissue samples exhibited significantly greater predicted hydrogen sulfide flux than normal but not adjacent samples (Fig. 6; with outliers – Supp. Fig. 4). These results aligned with the metabolomics results – significantly increased concentrations of the amino acid proxies for hydrogen sulfide on tumor tissue. To confirm this, we examined direct correlations between hydrogen sulfide flux (from the models) and amino acid concentrations in colon tissue (from metabolomics). Unexpectedly, we found that they were not correlated (Supp. Fig. 5). When we examined correlations between hydrogen sulfide flux and amino acid abundance in Fusobacterium alone the correlations were significant (Supp. Fig. 6). We then queried the models to identify the predicted microbes and reactions involved in hydrogen sulfide production. The models predicted that *Fusobacterium nucleatum*, *Clostridium perfringens,* and *Filifactor alocis* (formerly *Fusobacterium alocis* [62]) were significant hydrogen sulfide producers. Moreover, *B. fragilis* was observed to uptake and utilize this microbially-produced hydrogen sulfide in the models. Additionally, the dominant reaction predicted for hydrogen sulfide production was the cysteine degradation pathway catalyzed by L-cysteine desulfhydrase (L-cysteine + $H_2O \rightarrow$ pyruvate + hydrogen sulfide + ammonium), a pathway that did not involve any of the amino acid proxies we use to measure hydrogen sulfide production via metabolomics. While many microbial species contain this pathway, the models attributed the majority of hydrogen sulfide flux to *F. nucleatum*, *C. perfringens*, and *F. alocis.*

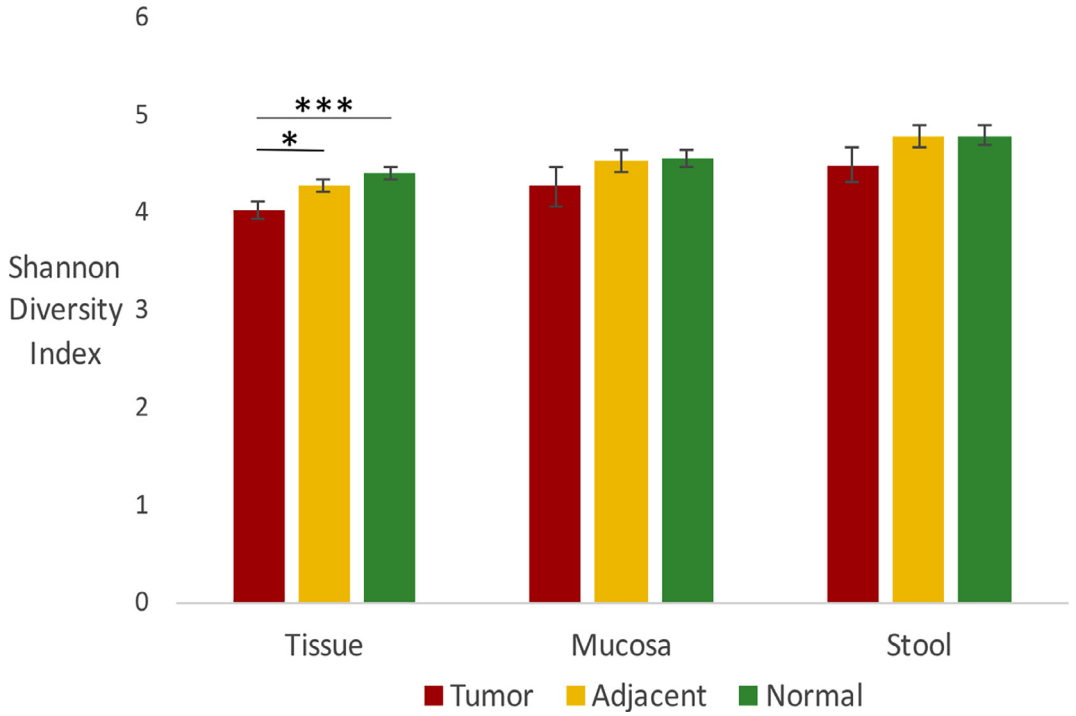

Fig. 1. Alpha-diversity of stool, colon tissue, and mucosa samples collected on and off the tumor site (plotted mean with SEM; *p < 0.05, ***p < 0.0001; Kruskal-Wallis with Dunn's post hoc tests; N = 107).

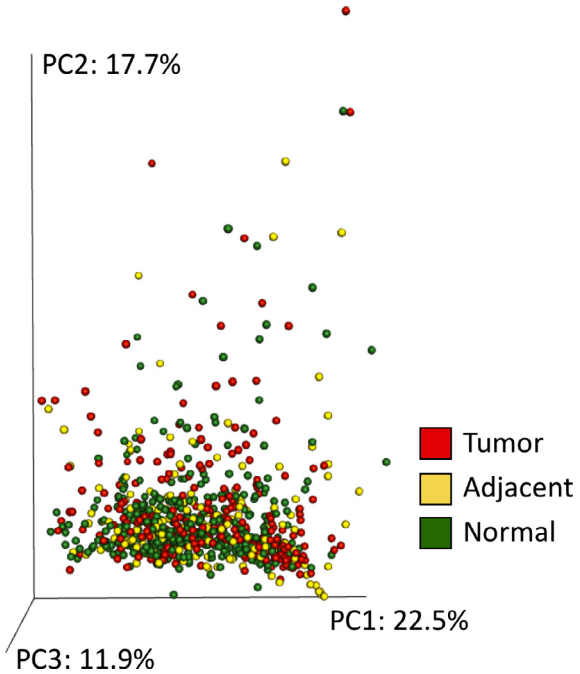

Fig. 2. Beta-diversity (weighted UniFrac) of stool, colon tissue, and mucosa samples collected on and off the tumor site (N = 107 individuals sampled).

4. Discussion

Our results provide several key insights into the interplay between microbes and metabolites in colorectal cancer. First, the combination of 16S and metabolomic data revealed that metabolite profiles but not microbial composition differed dramatically between tumor, adjacent, and normal samples. This suggests that metabolites—or community function—may be more important to evaluate than individual microbes or microbial composition in CRC pathogenesis. While 2 microbes, a hydrogen sulfide producing *Fusobacterium* species and *B. fragilis*, were significantly enriched in early stage tumor samples, several hundred metabolites were enriched in these same samples including amino acid proxies for hydrogen sulfide production (homoserine, lanthionine, cystathionine). These results suggest a role for hydrogen sulfide in CRC; although, the nature of that role is unclear based on these data alone. On one hand, hydrogen sulfide produced by *F. nucleatum* or other microbial species may be promoting tumorigenesis by damaging host cells and DNA. Indeed, *F. nucelatum* has well established mechanistic links to CRC tumor development [37,63–65], albeit, unrelated to hydrogen sulfide production. On the other hand, metabolomics profiles identify no source agent (host, microbe, microbial species). The community microbial metabolic models were able to predict specific microbial agents (*F. nucleatum, C. perfringens, F. alocis*) in relation to the increased hydrogen sulfide flux. However, hydrogen sulfide production could also be attributed to host pathways that are not accounted for in the models. In the host, hydrogen sulfide is generated as an anti-inflammatory agent; thus, it is feasible that this metabolite is elevated in tumor samples due to host tissue reaction to tumor-induced inflammation [26,66,67]. Further work is necessary to assess the source and role of hydrogen sulfide in relation to defined microbial communities and host tissue on and off tumor sites. Other factors that could potentially shape host or microbial community composition, expression, and interactions include tumor location and stage, patient medications (ranging from proton-pump inhibitors to antidepressants to statins and allergy medications) [68,69], smoking history [70], BMI [70], and surgical preparation (a subset of patients received MiraLAX preparation) [71]. We were unable to control for all of these variables due to lack of power; however, despite the variation in the patient population and tumor status, we detected consistent and significant differences in microbial and metabolomic profiles between tumor, adjacent, and normal colon. Additionally, this study design allowed each patient to serve as a control for him/herself as tumor, normal, and adjacent tissue within the same individual were all subject to the same factors (smoking, BMI, medications, surgical preparation).

A second key insight we gained from this work was the value of

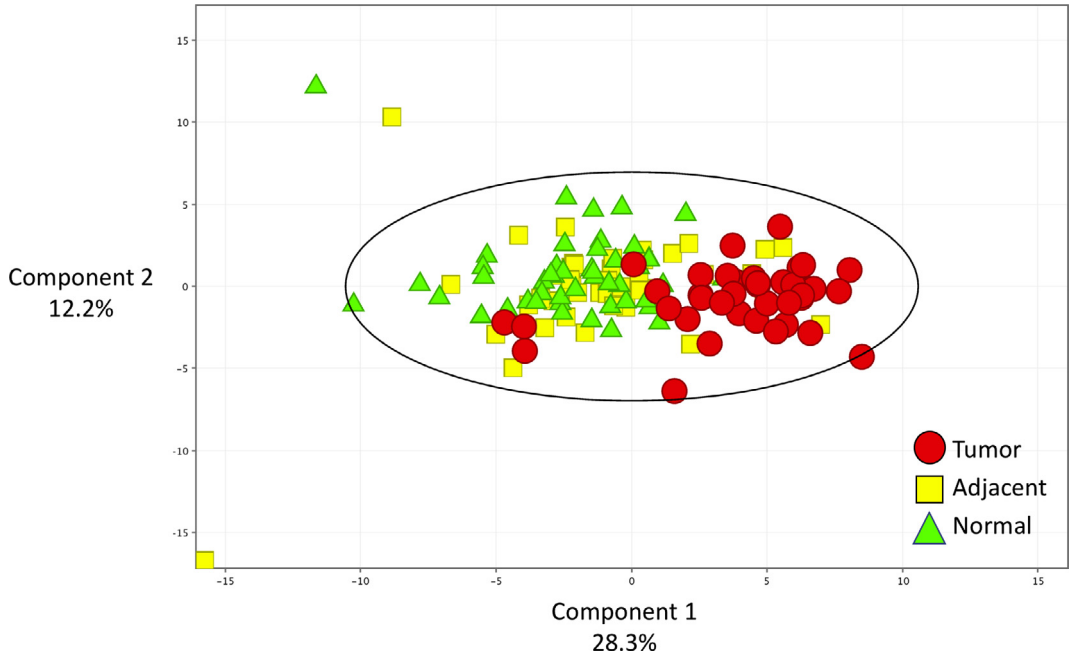

Fig. 3. Principal Component Analysis (PCA) of untargeted metabolomic profiles of colon tissue samples (N = 50 individuals). Stool and mucosa samples were not included in this analysis.

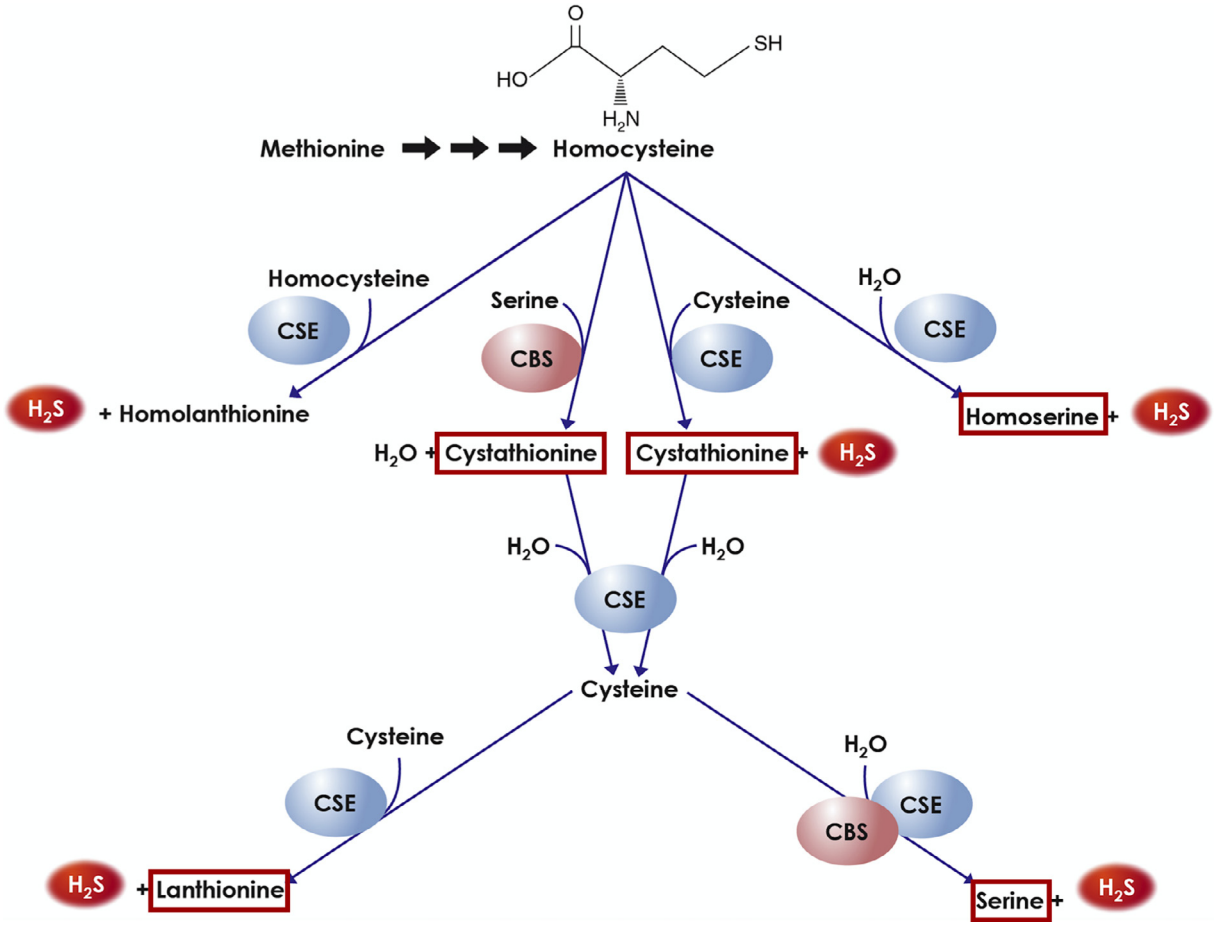

Fig. 4. Hydrogen sulfide production pathways. This study quantified concentrations of the metabolites in red boxes as proxies for hydrogen sulfide production. No standard was available for homolanthionine. Reprinted with permission of Caymen Chemical. (For interpretation of the references to colour in this figure legend, the reader is referred to the web version of this article.)

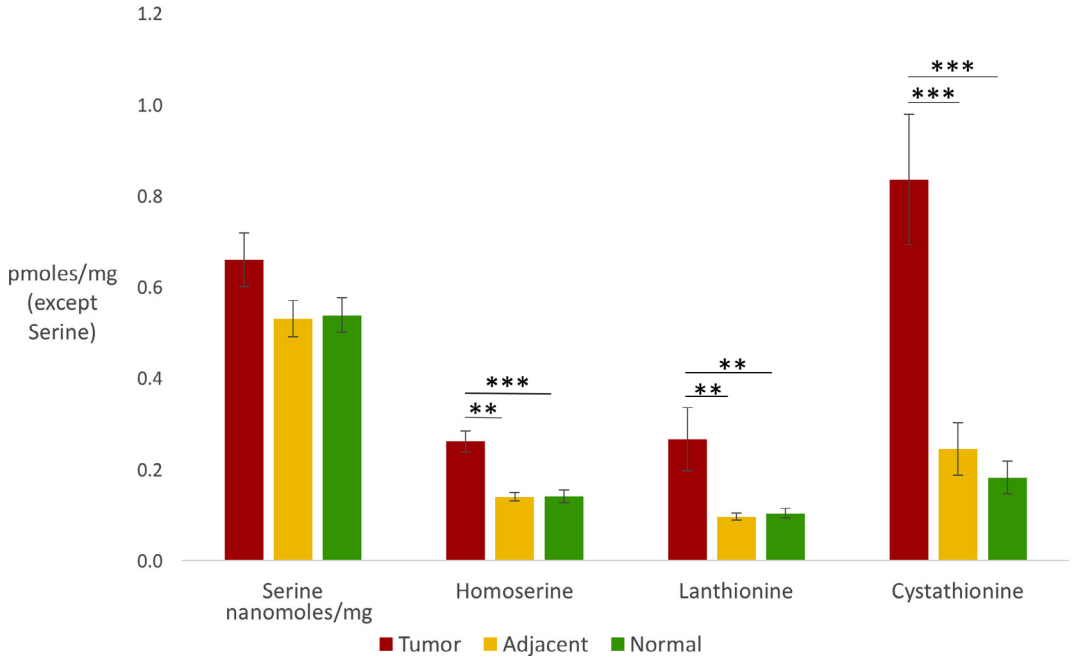

Fig. 5. Amino acid concentrations on and off tumor tissue. These amino acids serve as proxies for hydrogen sulfide production (plotted mean with SEM; **p < 0.01, ***p < 0.0001; Kruskal-Wallis with Dunn's post hoc tests; N = 44). Stool and mucosa samples were not included in this analysis.

using community metabolic models integrated with multi-omic data. The models allowed us to predict hydrogen sulfide flux through defined microbial communities and allowed us to examine the reactions, microbes, and microbial interactions underlying this flux. We made several important observations based on the models. First, the models predicted a feasible microbial basis for the increased hydrogen sulfide production in tumor tissue—a conclusion that was impossible to reach with 16S or metabolomic data alone. Although further *in vitro* and *in vivo* testing is required to confirm these predictions; ultimately, effective *in silico* modeling may provide us an alternate means of prediction when such testing is limited either by resources or by ethical considerations in human subjects. Second, metabolomic data appeared to serve as a strong validation of model predictions with both models and metabolomics identifying increased hydrogen sulfide production on tumor tissue. However, when we examined the direct relationship between metabolite profiles and hydrogen sulfide flux, we found no significant correlations until we narrowed our examination to *Fusobacterium* alone. This highlights the need to synthesize community metabolic modeling with 16S data for interpreting metabolomics results. This approach lead us to examine hydrogen sulfide production more closely in the models. We identified 2 other microbes (*C. perfringens* and *F. alocis*) and a reaction (cysteine degradation catalyzed by L-cysteine desulfhydrase) responsible for a large portion of the hydrogen sulfide production in the metabolic models. Both *C. perfringens* and *F. alocis* have demonstrated hydrogen sulfide production experimentally [72–74]. Clostridial species have additionally been associated with CRC in previous studies [75,76]. However, neither of these microbes was differentially abundant in 16S tumor samples, but the microbes could be functioning in different ways on and off the tumor site without varying in abundance, again underscoring the importance of

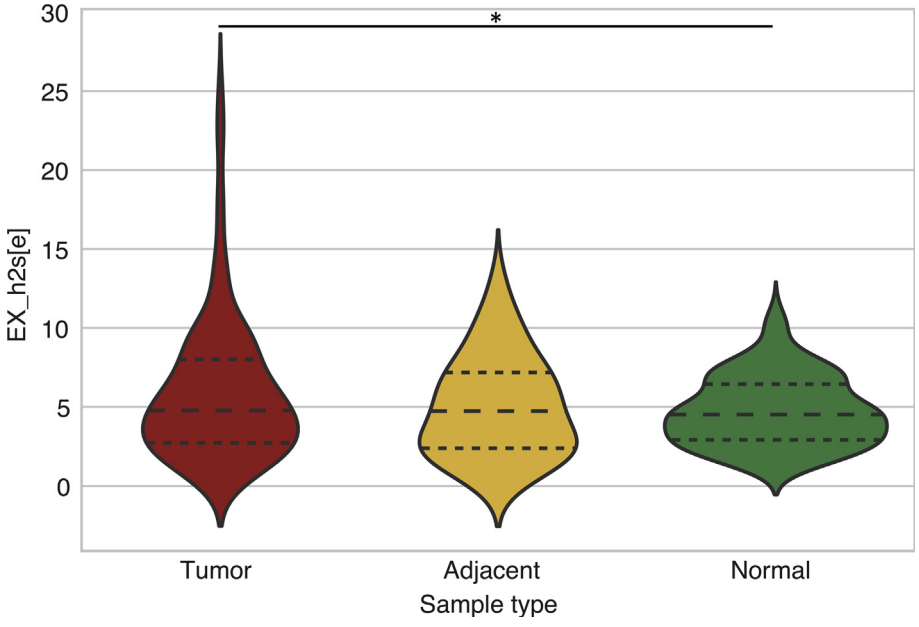

Fig. 6. Predicted hydrogen sulfide flux from colon tissue and mucosa microbial community metabolic models based on 16S relative abundances (*p < 0.05; Wilcoxon rank sum; n = 36 individuals, 241 samples). Three outliers that fell outside of the 95% confidence intervals were removed from this figure. See Supp. Fig. 4 for the figure with outliers present. Stool samples were not included in this analysis.

evaluating microbial metabolic function over single microbes or microbial composition. The L-cysteine desulfhydrase reaction was also an important discovery because it revealed that our metabolomic data potentially underestimated hydrogen sulfide production as we did not quantify any proxies for hydrogen sulfide in this pathway. A third important observation we made based on the models was a unique metabolic interaction involving hydrogen sulfide utilization by *B. fragilis*. The models predicted that if hydrogen-sulfide producing bacteria were present, *B. fragilis* and other *Bacteroides* species would consume that hydrogen sulfide; an interaction, to our knowledge, heretofore unidentified and unstudied. While multiple studies have demonstrated cross-feeding between *Bacteroides* species and other members of the gut microbial community—including sulfate-reducing bacteria [77,78]—no studies, to our knowledge, have demonstrated cross-feeding or metabolic exchange in relation to *F. nucleatum*, *C. perfringins*, *F. alocis* or hydrogen sulfide. In fact, the only microbes that have been identified as hydrogen sulfide utilizers appear to be environmental microbes [79–81]. As such, the validity of this predicted interaction, while intriguing, requires further investigation. Interestingly, both *F. nucleatum* and toxigenic *B. fragilis* are reported to be independent promoters of CRC tumorigenesis [37,61,63–65]. It is unknown what the effects of these interacting microbes may have together on tumorigenesis. Both *B. fragilis* and *Fusobacterium* were also identified in our 16S data and both were significantly enriched in early stage CRC. We further confirmed that the toxigenic strain of *B. fragilis* was present in 9% of the 98 individuals tested via qPCR. Co-culture experiments tracking hydrogen sulfide production and utilization between *B. fragilis* and *Fusobacterium* and *in vivo* testing of these microbes alone and together in gnotobiotic models could provide further insight into if and how these 2 oncogenic microbes interact.

As to why there was no correlation between models and metabolomics, there are a few possibilities:

- We were comparing apples to oranges and ideally should have measured and correlated hydrogen sulfide concentrations against hydrogen sulfide flux.
- The models are inaccurate. Models are only as good as their genome annotations, and many genomes can include inaccurate or missing annotations resulting in added or deleted reactions that fail to represent biological reality. Additionally, model assumptions, like the steady state assumption in MICOM, may fail to capture the changing dynamics of the colorectal cancer microbial community. Our assumption that hydrogen sulfide flux accurately predicts hydrogen sulfide production may also be flawed. Finally, these models do not include biological elements like host, diet, environment, or transcriptional regulation, all of which provide important context in the metabolic interactions of the gut. The models may have coincidentally predicted increased hydrogen sulfide flux in tumor tissue due to a heavy reliance on the cysteine degradation pathway when perhaps this pathway is not as active as predicted *in vivo*.
- The metabolomics are inaccurate. Perhaps the models accurately predicted high levels of hydrogen sulfide flux through the cysteine degradation pathway and our metabolomics data underestimates hydrogen sulfide levels by not including a proxy in this pathway. The metabolomics may have coincidentally predicted high levels of hydrogen sulfide production in tumor tissue due to increased host-produced anti-inflammatory hydrogen sulfide rather than microbially-produced hydrogen sulfide.

Each of these scenarios can be isolated and tested *in vitro* and *in vivo* to determine where biological "truth" actually lies. Additionally, to determine if we can produce a better metabolomic-model correlation, we could select and evaluate other microbial metabolites that can be directly quantified in both metabolomics and models (without proxies), and that cannot be attributed to host production.

Our study demonstrates one way in which metabolic models can be synthesized with multi–omic data in a complementary approach to hypothesis testing. As the ability to model complex biological interactions improves and is validated through laboratory experimentation, future modeling efforts may serve as even better predictors for metabolic interactions and disease conditions. Models and the tools built around these models are rapidly growing and improving and may eventually account for elements of host [82,83], diet, and transcriptional regulation. Many community modeling approaches like MICOM assess flux, and here we use flux to approximate metabolite production. Further developments in modeling may eventually allow us to predict metabolite production more directly by incorporating varying rates of enzyme activity. For example, in the following reaction, enzyme X catalyzes the reaction from metabolite A to B and enzyme Y catalyzes the reaction from B to C.

$$A \xrightarrow{X} B \xrightarrow{Y} C$$

If X has a faster reaction rate than Y, then metabolite B will accumulate in the system. If Y has a faster reaction rate than X, then metabolite C will accumulate in the system. Incorporating and tracking these reaction rates could allow future models to infer metabolite profiles more effectively. Advances like this will improve our ability to maximize multi-omic data potential in combination with metabolic modeling.

5. Conclusions

Here, we used experimental data (16S) to inform genome-scale community metabolic models; models to test a hypothesis about hydrogen sulfide production and CRC; experimental data (metabolomics) to assess model output; and modeling data to guide future work on specific metabolic reactions and microbial metabolic interactions. We draw 5 main conclusions from our work:

1. Hydrogen sulfide production is increased in CRC tumor samples, and this hydrogen sulfide has several potential sources including host or microbes predicted by both 16S and modeling data.
2. Microbial metabolic function or community interactions may be more important to evaluate than single microbes or microbial composition in CRC pathogenesis.
3. Metabolic modeling is a rapidly developing and inexpensive way to establish early predictions about community function and interactions that can guide future work.
4. A word of warning: Modeling can fail to represent biological reality. Assess accuracy of models in your respective systems and be aware that models and reactions can be altered (i.e. added, removed) to improve accuracy.
5. Synthesis of multi-omic data and microbial community metabolic models allows maximization of data potential for hypothesis testing and hypothesis generation.

Acknowledgements

First and foremost, we thank the patients who volunteered for this study. Each measured step of our research is performed with the greater goal of improving our ability to prevent, diagnose, and treat colorectal cancer, and that research would not be possible without our patients. We also gratefully acknowledge all of the many other individuals who made this research possible – from study coordinators to students, to surgeons, to program directors, to pathology assistants and laboratory technicians. We also acknowledge the reviewers for their helpful comments that improved this manuscript. Funding was provided by the NIH (R01CA179243; N.C. and V.L.H. and R01CA170357; L.B.), the Mayo Clinic Center for Cell Signaling in Gastroenterology (NIDDK P30DK084567), the Mayo Clinic Metabolomics Resource Core Pilot and Feasibility Award (U24DK100469), the Fred C. Andersen Foundation

(H.N. and N.C.), and the Mayo Clinic Center for Individualized Medicine. O.R.A thanks the financial support coming from the National Institute of Genomic Medicine (INMEGEN) to develop the computational tool used for the microbiome analysis (MICOM).

Appendix A. Supplementary data

Supplementary data associated with this article can be found, in the online version, at http://dx.doi.org/10.1016/j.ymeth.2018.04.024.

References

[1] M.L. Jenior, J.L. Leslie, V.B. Young, P.D. Schloss, Clostridium difficile colonizes alternative nutrient niches during infection across distinct murine gut microbiomes, mSystems 2 (4) (2017) e00063-17.
[2] J. Sung, S. Kim, J.J.T. Cabatbat, S. Jang, Y.-S. Jin, G.Y. Jung, N. Chia, P.-J. Kim, Global metabolic interaction network of the human gut microbiota for context-specific community-scale analysis, Nat. Commun. 8 (2017) 15393.
[3] R.A. Koeth, Z. Wang, B.S. Levison, J.A. Buffa, E. Org, B.T. Sheehy, E.B. Britt, X. Fu, Y. Wu, L. Li, J.D. Smith, J.A. DiDonato, J. Chen, H. Li, G.D. Wu, J.D. Lewis, M. Warrier, J.M. Brown, R.M. Krauss, W.H.W. Tang, F.D. Bushman, A.J. Lusis, S.L. Hazen, Intestinal microbiota metabolism of l-carnitine, a nutrient in red meat, promotes atherosclerosis, Nat. Med. 19 (5) (2013) 576–585.
[4] A. Gomez, K. Petrzelkova, C.J. Yeoman, K. Vlckova, J. Mrázek, I. Koppova, F. Carbonero, A. Ulanov, D. Modry, A. Todd, M. Torralba, K.E. Nelson, H.R. Gaskins, B. Wilson, R.M. Stumpf, B.A. White, S.R. Leigh, Gut microbiome composition and metabolomic profiles of wild western lowland gorillas (Gorilla gorilla gorilla) reflect host ecology, Mol. Ecol. 24 (10) (2015) 2551–2565.
[5] C.M. Theriot, M.J. Koenigsknecht, P.E. Carlson, G.E. Hatton, A.M. Nelson, B. Li, G.B. Huffnagle, J. Li, V.B. Young, Antibiotic-induced shifts in the mouse gut microbiome and metabolome increase susceptibility to Clostridium difficile infection, Nat. Commun. 5 (2014) 3114.
[6] V.C. Antharam, D.C. McEwen, T.J. Garrett, A.T. Dossey, E.C. Li, A.N. Kozlov, Z. Mesbah, G.P. Wang, An integrated metabolomic and microbiome analysis identified specific gut microbiota associated with fecal cholesterol and coprostanol in clostridium difficile infection, PLOS ONE 11 (2) (2016) e0148824.
[7] E.A. Franzosa, X.C. Morgan, N. Segata, L. Waldron, J. Reyes, A.M. Earl, G. Giannoukos, M.R. Boylan, D. Ciulla, D. Gevers, J. Izard, W.S. Garrett, A.T. Chan, C. Huttenhower, Relating the metatranscriptome and metagenome of the human gut, Proc. Nat. Acad. Sci. 111 (22) (2014) E2329–E2338.
[8] J. Kamke, S. Kittelmann, P. Soni, Y. Li, M. Tavendale, S. Ganesh, P.H. Janssen, W. Shi, J. Froula, E.M. Rubin, G.T. Attwood, Rumen metagenome and metatranscriptome analyses of low methane yield sheep reveals a Sharpea-enriched microbiome characterised by lactic acid formation and utilisation, Microbiome 4 (1) (2016) 56.
[9] J. Sung, V. Hale, A.C. Merkel, P.-J. Kim, N. Chia, Metabolic modeling with Big Data and the gut microbiome, Appl. Transl. Genomics 10 (2016) 10–15.
[10] American Cancer Society, Colorectal cancer facts & figures 2014-2016, 2014. http://www.cancer.org/acs/groups/content/documents/document/acspc-042280.pdf.
[11] P. Louis, G.L. Hold, H.J. Flint, The gut microbiota, bacterial metabolites and colorectal cancer, Nat. Rev. Micro. 12 (10) (2014) 661–672.
[12] M.S. Attene-Ramos, G.M. Nava, M.G. Muellner, E.D. Wagner, M.J. Plewa, H.R. Gaskins, DNA damage and toxicogenomic analyses of hydrogen sulfide in human intestinal epithelial FHs 74 Int cells, Environ. Mol. Mutagen 51 (4) (2010) 304–314.
[13] M.S. Attene-Ramos, E.D. Wagner, H.R. Gaskins, M.J. Plewa, Hydrogen Sulfide Induces Direct Radical-Associated DNA Damage, Mol. Cancer Res. 5 (5) (2007) 455–459.
[14] N. Reichardt, S.H. Duncan, P. Young, A. Belenguer, C.M. Leitch, K.P. Scott, H.J. Flint, P. Louis, Phylogenetic distribution of three pathways for propionate production within the human gut microbiota, ISME J. 8 (2014).
[15] Y.H. Loh, P. Jakszyn, R.N. Luben, A.A. Mulligan, P.N. Mitrou, K.-T. Khaw, N-nitroso compounds and cancer incidence: the European Prospective Investigation into Cancer and Nutrition (EPIC)–Norfolk Study, Am. J. Clinical Nutrition 93 (5) (2011) 1053–1061.
[16] A.E. Pegg, Toxicity of polyamines and their metabolic products, Chem. Res. Toxicol. 26 (12) (2013) 1782–1800.
[17] J.M. Ridlon, P.G. Wolf, H.R. Gaskins, Taurocholic acid metabolism by gut microbes and colon cancer, Gut Microbes 7 (3) (2016) 201–215.
[18] C. Bernstein, H. Holubec, A.K. Bhattacharyya, H. Nguyen, C.M. Payne, B. Zaitlin, H. Bernstein, Carcinogenicity of deoxycholate, a secondary bile acid, Arch. Toxicol. 85 (8) (2011) 863–871.
[19] A. Belcheva, T. Irrazabal, Susan J. Robertson, C. Streutker, H. Maughan, S. Rubino, Eduardo H. Moriyama, Julia K. Copeland, A. Surendra, S. Kumar, B. Green, K. Geddes, Rossanna C. Pezo, William W. Navarre, M. Milosevic, Brian C. Wilson, Stephen E. Girardin, Thomas M.S. Wolever, W. Edelmann, David S. Guttman, Dana J. Philpott, A. Martin, Gut microbial metabolism drives transformation of msh2-deficient colon epithelial cells, Cell 158 (2) (2014) 288–299.
[20] S.J. Bultman, Molecular pathways: gene-environment interactions regulating dietary fiber induction of proliferation and apoptosis via butyrate for cancer prevention, Clin. Cancer Res. 20 (4) (2014) 799–803.
[21] V.L. Hale, J. Chen, S. Johnson, S.C. Harrington, T.C. Yab, T.C. Smyrk, H. Nelson, L. A. Boardman, B.R. Druliner, T.R. Levin, D.K. Rex, D.J. Ahnen, P. Lance, D.A. Ahlquist, N. Chia, Shifts in the fecal microbiota associated with adenomatous polyps, Cancer Epidemiology Biomarkers & Prevention, 2016.
[22] W.-J. Cai, M.-J. Wang, L.-H. Ju, C. Wang, Y.-C. Zhu, Hydrogen sulfide induces human colon cancer cell proliferation: Role of Akt, ERK and p21, Cell Biol. Int. 34 (6) (2010) 565–572.
[23] C. Szabo, C. Coletta, C. Chao, K. Módis, B. Szczesny, A. Papapetropoulos, M.R. Hellmich, Tumor-derived hydrogen sulfide, produced by cystathionine-β-synthase, stimulates bioenergetics, cell proliferation, and angiogenesis in colon cancer, PNAS 110 (30) (2013) 12474–12479.
[24] M.S. Attene-Ramos, E.D. Wagner, M.J. Plewa, H.R. Gaskins, Evidence that hydrogen sulfide is a genotoxic agent, Mol. Cancer Res. 4 (1) (2006) 9–14.
[25] G. Yang, Hydrogen sulfide in cell survival: a double-edged sword, Expert Rev. Clin. Pharmacol. 4 (1) (2011) 33–47.
[26] B. Gemici, J.L. Wallace, Chapter Nine – Anti-inflammatory and cytoprotective properties of hydrogen sulfide, in: E. Cadenas, L. Packer (Eds.), Methods in Enzymology, Academic Press, 2015, pp. 169–193.
[27] M. Chattopadhyay, R. Kodela, K.R. Olson, K. Kashfi, NOSH–aspirin (NBS-1120), a novel nitric oxide- and hydrogen sulfide-releasing hybrid is a potent inhibitor of colon cancer cell growth in vitro and in a xenograft mouse model, Biochem. Biophys. Res. Commun. 419 (3) (2012) 523–528.
[28] M. Chattopadhyay, R. Kodela, N. Nath, Y.M. Dastagirzada, C.A. Velázquez-Martínez, D. Boring, K. Kashfi, Hydrogen sulfide-releasing NSAIDs inhibit the growth of human cancer cells: a general property and evidence of a tissue type-independent effect, Biochem. Pharmacol. 83 (6) (2012) 715–722.
[29] K. Kashfi, Anti-cancer activity of new designer hydrogen sulfide-donating hybrids, Antioxid. Redox Signal. 20 (5) (2014) 831–846.
[30] J.L. Wallace, M. Dicay, W. McKnight, G.R. Martin, Hydrogen sulfide enhances ulcer healing in rats, FASEB J. 21 (14) (2007) 4070–4076.
[31] D.R. Linden, M.D. Levitt, G. Farrugia, J.H. Szurszewski, Endogenous production of h (2)s in the gastrointestinal tract: still in search of a physiologic function, Antioxid. Redox Signal. 12 (9) (2010) 1135–1146.
[32] S. Devkota, Y. Wang, M.W. Musch, V. Leone, H. Fehlner-Peach, A. Nadimpalli, D.A. Antonopoulos, B. Jabri, E.B. Chang, Dietary-fat-induced taurocholic acid promotes pathobiont expansion and colitis in Il10$^{-/-}$ mice, Nat 487 (7405) (2012) 104–108.
[33] A.N. McCoy, F. Araujo-Perez, A. Azcarate-Peril, J.J. Yeh, R.S. Sandler, T.O. Keku, Fusobacterium is associated with colorectal adenomas, PLoS ONE 8 (1) (2013) e53653.
[34] L. Mira-Pascual, R. Cabrera-Rubio, S. Ocon, P. Costales, A. Parra, A. Suarez, F. Moris, L. Rodrigo, A. Mira, M.C. Collado, Microbial mucosal colonic shifts associated with the development of colorectal cancer reveal the presence of different bacterial and archaeal biomarkers, J. Gastroenterol. 50 (2) (2014) 167–179.
[35] J.P. Zackular, N.T. Baxter, K.D. Iverson, W.D. Sadler, J.F. Petrosino, G.Y. Chen, P.D. Schloss, The gut microbiome modulates colon tumorigenesis, mBio. 4 (6) (2013) 13.
[36] M. Castellarin, R.L. Warren, J.D. Freeman, L. Dreolini, M. Krzywinski, J. Strauss, R. Barnes, P. Watson, E. Allen-Vercoe, R.A. Moore, R.A. Holt, Fusobacterium nucleatum infection is prevalent in human colorectal carcinoma, Genome Res. 22 (2) (2012) 299–306.
[37] J. Abed, J.E.M. Emgård, G. Zamir, M. Faroja, G. Almogy, A. Grenov, A. Sol, R. Naor, E. Pikarsky, K.A. Atlan, A. Mellul, S. Chaushu, A.L. Manson, A.M. Earl, N. Ou, C.A. Brennan, W.S. Garrett, G. Bachrach, Fap2 mediates fusobacterium nucleatum colorectal adenocarcinoma enrichment by binding to tumor-expressed Gal-GalNAc, Cell Host Microbe 20 (2) (2016) 215–225.
[38] H. Mendes-Soares, M. Mundy, L.M. Soares, N. Chia, MMinte: an application for predicting metabolic interactions among the microbial species in a community, BMC Bioinf. 17 (1) (2016) 343.
[39] S.H.J. Chan, M.N. Simons, C.D. Maranas, SteadyCom: pmicrobial abundances while ensuring community stability, PLOS Comput. Biol. 13 (5) (2017) e1005539.
[40] A.R. Zomorrodi, C.D. Maranas, OptCom: a multi-level optimization framework for the metabolic modeling and analysis of microbial communities, PLoS Comput Biol 8 (2012).
[41] C. Zhang, Q. Hua, Applications of genome-scale metabolic models in biotechnology and systems medicine, Front. Physiol. 6 (413) (2016).
[42] J.D. Orth, I. Thiele, B.O. Palsson, What is flux balance analysis? Nat Biotechnol 28 (3) (2010) 245–248.
[43] C. Diener, O. Resendis-Antonio, MICOM, 2017. https://github.com/resendislab/micom. (Accessed September 2017).
[44] E.A. Baldwin, M. Walther-Antonio, A.M. MacLean, D.M. Gohl, K.B. Beckman, J. Chen, B. White, D.J. Creedon, N. Chia, Persistent microbial dysbiosis in preterm premature rupture of membranes from onset until delivery, PeerJ. 3 (2015) e1398.
[45] P. Jeraldo, K. Kalari, X. Chen, J. Bhavsar, A. Mangalam, B. White, H. Nelson, J.-P. Kocher, N. Chia, IM-TORNADO: A tool for comparison of 16S reads from paired-end libraries, PLoS ONE 9 (12) (2014) e114804.
[46] J.G. Caporaso, K. Bittinger, F.D. Bushman, T.Z. DeSantis, G.L. Andersen, R. Knight, PyNAST: a flexible tool for aligning sequences to a template alignment, Bioinformatics 26 (2) (2010) 266–267.
[47] J.G. Caporaso, J. Kuczynski, J. Stombaugh, K. Bittinger, F.D. Bushman, E.K. Costello, N. Fierer, A.G. Peña, J.K. Goodrich, J.I. Gordon, G.A. Huttley, S.T. Kelley, D. Knights, J.E. Koenig, R.E. Ley, C.A. Lozupone, D. McDonald, B.D. Muegge, M. Pirrung, J. Reeder, J.R. Sevinsky, P.J. Turnbaugh, W.A. Walters, J. Widmann, T. Yatsunenko, J. Zaneveld, R. Knight, QIIME allows analysis of high-throughput community sequencing data, Nat. Methods 7 (5) (2010) 335–336.
[48] R.V. Purcell, J. Pearson, F.A. Frizelle, J.I. Keenan, Comparison of standard,

quantitative and digital PCR in the detection of enterotoxigenic Bacteroides fragilis, Sci. Rep. 6 (2016) 34554.
[49] I.R. Lanza, S. Zhang, L.E. Ward, H. Karakelides, D. Raftery, K.S. Nair, Quantitative metabolomics by 1H-NMR and LC-MS/MS confirms altered metabolic pathways in diabetes, PLOS ONE 5 (5) (2010) e10538.
[50] N.M. Moreau, S.M. Goupry, J.P. Antignac, F.J. Monteau, B.J. Le Bizec, M.M. Champ, L.J. Martin, H.J. Dumon, Simultaneous measurement of plasma concentrations and 13C-enrichment of short-chain fatty acids, lactic acid and ketone bodies by gas chromatography coupled to mass spectrometry, J. Chromatogr. B 784 (2) (2003) 395–403.
[51] T. Dutta, H.S. Chai, L.E. Ward, A. Ghosh, X.-M.T. Persson, G.C. Ford, Y.C. Kudva, Z. Sun, Y.W. Asmann, J.-P.A. Kocher, K.S. Nair, Concordance of changes in metabolic pathways based on plasma metabolomics and skeletal muscle transcriptomics in type 1 diabetes, Diabetes 61 (5) (2012) 1004–1016.
[52] E. Trushina, T. Dutta, X.-M.T. Persson, M.M. Mielke, R.C. Petersen, Identification of altered metabolic pathways in plasma and CSF in mild cognitive impairment and alzheimer's disease using metabolomics, PLOS ONE 8 (5) (2013) e63644.
[53] T. Dutta, Y.C. Kudva, X.-M.T. Persson, L.A. Schenck, G.C. Ford, R.J. Singh, R. Carter, K.S. Nair, Impact of long-term poor and good glycemic control on metabolomics alterations in type 1 diabetic people, J. Clin. Endocrinol. Metabolism 101 (3) (2016) 1023–1033.
[54] E. Fahy, S. Subramaniam, R.C. Murphy, M. Nishijima, C.R.H. Raetz, T. Shimizu, F. Spener, G. van Meer, M.J.O. Wakelam, E.A. Dennis, Update of the LIPID MAPS comprehensive classification system for lipids, J. Lipid Res. 50 (Suppl) (2009) S9–S14.
[55] J.G. Caporaso, C.L. Lauber, E.K. Costello, D. Berg-Lyons, A. Gonzalez, J. Stombaugh, D. Knights, P. Gajer, J. Ravel, N. Fierer, J.I. Gordon, R. Knight, Moving pictures of the human microbiome, Genome Biol. 12 (5) (2011) R50.
[56] S. Magnusdottir, A. Heinken, L. Kutt, D.A. Ravcheev, E. Bauer, A. Noronha, K. Greenhalgh, C. Jager, J. Baginska, P. Wilmes, R.M.T. Fleming, I. Thiele, Generation of genome-scale metabolic reconstructions for 773 members of the human gut microbiota, Nat. Biotech. 35 (1) (2017) 81–89.
[57] A. Bankevich, S. Nurk, D. Antipov, A.A. Gurevich, M. Dvorkin, A.S. Kulikov, V.M. Lesin, S.I. Nikolenko, S. Pham, A.D. Prjibelski, A.V. Pyshkin, A.V. Sirotkin, N. Vyahhi, G. Tesler, M.A. Alekseyev, P.A. Pevzner, SPAdes: a new genome assembly algorithm and its applications to single-cell sequencing, J. Comput. Biol. 19 (5) (2012) 455–477.
[58] R.R. Wick, L.M. Judd, C.L. Gorrie, K.E. Holt, Unicycler: resolving bacterial genome assemblies from short and long sequencing reads, PLOS Comput. Biol. 13 (6) (2017) e1005595.
[59] T. Rognes, T. Flouri, B. Nichols, C. Quince, F. Mahé, VSEARCH: a versatile open source tool for metagenomics, PeerJ 4 (2016) e2584.
[60] A. Boleij, E.M. Hechenbleikner, A.C. Goodwin, R. Badani, E.M. Stein, M.G. Lazarev, B. Ellis, K.C. Carroll, E. Albesiano, E.C. Wick, E.A. Platz, D.M. Pardoll, C.L. Sears, The bacteroides fragilis toxin gene is prevalent in the colon mucosa of colorectal cancer patients, Clin. Infectious Dis.: Off. Publ. Infectious Dis. Soc. Am. 60 (2) (2015) 208–215.
[61] S. Wu, K.-J. Rhee, E. Albesiano, S. Rabizadeh, X. Wu, H.-R. Yen, D.L. Huso, F.L. Brancati, E. Wick, F. McAllister, F. Housseau, D.M. Pardoll, C.L. Sears, A human colonic commensal promotes colon tumorigenesis via activation of T helper type 17 T cell responses, Nat Med 15 (9) (2009) 1016–1022.
[62] A.W. Aruni, A. Mishra, Y. Dou, O. Chioma, B.N. Hamilton, H.M. Fletcher, Filifactor alocis — a new emerging periodontal pathogen, Microbes Infection/Institut Pasteur 17 (7) (2015) 517–530.
[63] A.D. Kostic, E. Chun, L. Robertson, J.N. Glickman, C.A. Gallini, M. Michaud, T.E. Clancy, D.C. Chung, P. Lochhead, G.L. Hold, E.M. El-Omar, D. Brenner, C.S. Fuchs, M. Meyerson, W.S. Garrett, Fusobacterium nucleatum Potentiates Intestinal Tumorigenesis and Modulates the Tumor-Immune Microenvironment, Cell Host Microbe 14 (2) (2013) 207–215.
[64] M.R. Rubinstein, X. Wang, W. Liu, Y. Hao, G. Cai, Y.W. Han, Fusobacterium nucleatum promotes colorectal carcinogenesis by modulating E-cadherin/β-catenin signaling via its FadA adhesin, Cell host & microbe 14 (2) (2013) 195–206.
[65] C. Gur, Y. Ibrahim, B. Isaacson, R. Yamin, J. Abed, M. Gamliel, J. Enk, Y. Bar-On, N. Stanietsky-Kaynan, S. Coppenhagen-Glazer, N. Shussman, G. Almogy, A. Cuapio, E. Hofer, D. Mevorach, A. Tabib, R. Ortenberg, G. Markel, K. Miklić, S. Jonjic, C.A. Brennan, W.S. Garrett, G. Bachrach, O. Mandelboim, Binding of the Fap2 Protein of *Fusobacterium nucleatum* to Human Inhibitory Receptor TIGIT Protects Tumors from Immune Cell Attack, Immunity 42 (2) (2015) 344–355.
[66] J.L. Wallace, R. Wang, Hydrogen sulfide-based therapeutics: exploiting a unique but ubiquitous gasotransmitter, Nat. Rev. Drug Discov. 14 (5) (2015) 329–345.
[67] K. Wang, M. Karin, Chapter Five – Tumor-elicited inflammation and colorectal cancer, in: X.-Y. Wang, P.B. Fisher (Eds.), Advances in Cancer Research, Academic Press, 2015, pp. 173–196.
[68] C.T. Seto, P. Jeraldo, R. Orenstein, N. Chia, J.K. DiBaise, Prolonged use of a proton pump inhibitor reduces microbial diversity: implications for Clostridium difficile susceptibility, Microbiome 2 (2014) 42.
[69] J.A. Caparrós-Martín, R.R. Lareu, J.P. Ramsay, J. Peplies, F. Jerry Reen, H.A. Headlam, N.C. Ward, K.D. Croft, P. Newsholme, J.D. Hughes, F. O'Gara, Statin therapy causes gut dysbiosis in mice through a PXR-dependent mechanism, Microbiome 5 (2017) 95.
[70] J. Chen, E. Ryu, M. Hathcock, K. Ballman, N. Chia, J.E. Olson, H. Nelson, Impact of demographics on human gut microbial diversity in a US Midwest population, PeerJ 4 (2016) e1514.
[71] C.L. O'Brien, G.E. Allison, F. Grimpen, P. Pavli, Impact of Colonoscopy Bowel Preparation on Intestinal Microbiota, PLOS ONE 8 (5) (2013) e62815.
[72] S. Persson, M.B. Edlund, R. Claesson, J. Carlsson, The formation of hydrogen sulfide and methyl mercaptan by oral bacteria, Oral Microbiol. Immunol. 5 (4) (2007) 195–201.
[73] R. Jame, V. Vilímová, B. Lakatoš, Ľ. Varečka, The hydrogen production by anaerobic bacteria grown on glucose and glycerol, Acta Chimica Slovaca 4 (2011) 2.
[74] A.-R. Fuchs, G.J. Bonde, The availability of sulphur for clostridium perfringens and an examination of hydrogen sulphide production, Microbiology 16 (2) (1957) 330–340.
[75] S. Melnick, S. Nazir, B. Chwiecko, B. Lloyd, There may be more than meets the eye with Clostridium perfringens bacteremia, J. Community Hospital Internal Med. Perspectives 7 (2) (2017) 134–135.
[76] B. Benjamin, M. Kan, D. Schwartz, Y. Siegman-Igra, The possible significance of Clostridium spp. in blood cultures, Clin. Microbiol. Infect. 12 (10) (2006) 1006–1012.
[77] F.E. Rey, Metabolic niche of a prominent sulfate-reducing human gut bacterium, Proc. Natl. Acad. Sci. USA 110 (2013).
[78] F. Turroni, C. Milani, S. Duranti, J. Mahony, D. van Sinderen, M. Ventura, Glycan utilization and cross-feeding activities by bifidobacteria, Trends Microbiol. (2017).
[79] R. Singh, S.K. Mandal, Microbial Removal of Hydrogen Sulfide from Biogas, Energy Sources Part A 34 (4) (2011) 306–315.
[80] M. Syed, G. Soreanu, P. Falletta, M. Béland, Removal of hydrogen sulfide from gas streams using biological processes – a review, Canad. Biosyst. Eng. 48 (2006) 2.1–2.14.
[81] J.M.M. de Zwart, J.G. Kuenen, Aerobic conversion of dimethyl sulfide and hydrogen sulfide by *Methylophaga sulfidovouans*: implications for modeling DMS conversion in a microbial mat, FEMS Microbiol. Ecol. 22 (1996) 155–165.
[82] E. Brunk, S. Sahoo, D.C. Zielinski, A. Altunkaya, A. Dräger, N. Mih, F. Gatto, A. Nilsson, G.A. Preciat Gonzalez, M.K. Aurich, A. Prlić, A. Sastry, A.D. Danielsdottir, A. Heinken, A. Noronha, P.W. Rose, S.K. Burley, R.M.T. Fleming, J. Nielsen, I. Thiele, B.O. Palsson, Recon3D enables a three-dimensional view of gene variation in human metabolism, Nat. Biotechnol. 36 (2018) 272.
[83] I. Thiele, S. Sahoo, A. Heinken, L. Heirendt, M.K. Aurich, A. Noronha, R.M.T. Fleming, When metabolism meets physiology: Harvey and Harvetta, bioRxiv, 2018.